

Gold as a Potential Contrast Agent for Dual-Energy CT

Radko Krissak, Martin Elgert, Björn Kusch, Ralph Hünerbein

Department of Diagnostic and Interventional Radiology, Hufeland Klinikum GmbH, Bad Langensalza, Germany
Email: r.krissak@hufeland.de

Received July 20, 2013; revised August 20, 2013; accepted August 27, 2013

Copyright © 2013 Radko Krissak *et al.* This is an open access article distributed under the Creative Commons Attribution License, which permits unrestricted use, distribution, and reproduction in any medium, provided the original work is properly cited.

ABSTRACT

Purpose: The K-edge of gold (81 keV) is located within the energy range of diagnostic CT. This might be advantageous for material differentiation in dual-energy CT (DECT). The aim of this *in vitro* study was to compare the differentiation between iodine or gold and body tissues using DECT at different kV spectra. **Methods and Materials:** A water filled tank phantom containing specimens with iodine (iopamidol), gold (sodium aurothiomalate), compact bone (compact porcine bone) and porcine muscle was scanned using a dual source CT (Definition, Siemens Healthcare). Consecutive scans were performed at 80 kVp, 100 kVp, 120 kVp and 140 kVp with constant mAs settings. The mean attenuation values of the specimens were measured, and differences in calculated dual-energy ratios (DE_{ratio}) between body tissues and iodine or gold were determined for different DE spectra. **Results:** The attenuation of gold increased compared to 80 kVp at higher kVp-settings, while the attenuation of all other specimens decreased. The calculated DE_{ratio} at 80/100 kVp, 80/120 kVp and 80/140 kVp were 1.31, 1.62 and 1.91 for iodine, 0.89, 0.88 and 0.92 for gold, 1.20, 1.39 and 1.45 for compact bone, 1.01, 1.03 and 1.08 for muscle. The differences between the DE_{ratio} 80/100 kVp, 80/120 kVp and 80/140 kVp were 0.11, 0.23 and 0.46 for iodine and bone, 0.31, 0.51 and 0.53 for gold and bone, 0.29, 0.59 and 0.83 for iodine and muscle, 0.12, 0.15 and 0.16 for gold and muscle. **Conclusion:** DE_{ratio} of gold remains relatively stable along the energy spectrum of diagnostic CT and allows a reliable material differentiation between gold and bone already at contiguous low tube voltage settings (80 kV and 100 kV). Thus, gold might have a potential as a contrast agent for DECT.

Keywords: Gold; Computed Tomography; Dual-Energy; Contrast Agent; K-Edge

1. Introduction

Materials can be differentiated by applying different X-ray spectra and analyzing the differences in attenuation [1-3]. This works especially well in materials with large atomic numbers due to the photo effect. Iodine is commonly used in CT as a contrast material and is generally known to have stronger enhancement at low tube voltage settings [4,5]. Selective iodine imaging using dual energy CT (DECT) was proposed already by Hounsfield [6] and further investigated in the late 1970s [3,7,8]. It was considered to perform dual energy imaging at energies around the iodine K edge (33 keV) [6], which would allow good iodine separation at contiguous tube voltages and thus similar noise levels. However, the radiation dose of patients would not be acceptable at such low energies. Additionally, technical limitations of the CT scanners at that time prevented the development of routine clinical applications [9].

Recent generations of high-end multidetector CTs are able to acquire DECT data by applying two X-ray tubes

and two corresponding detectors at different kVp and mA settings simultaneously in a dual-source CT (Siemens) [10], by ultra-fast kVp switching in a single-source CT (GE) [11] or by compartmentalization of detected X-ray photons into energy bins by the detectors of a single-source CT operating at constant kVp and mA settings (Philips) [12]. The ability to discriminate between two materials in DECT relies primarily on the difference between the dual energy ratios (DE_{ratio}) of the materials, which is determined by the separation between the high- and low-energy spectra and the difference between the atomic numbers of the evaluated materials. The smaller the spectral separation, the harder it is to discriminate between two materials [13].

DECT on a dual-source CT is typically performed using 80 and 140 kV spectra or 100 and 140 kV spectra in larger patients [14]. This results in relatively large image noise difference between the datasets, which is usually compensated by using different mAs settings for both tubes [10]. As mentioned above, it would be desirable to

perform the scans at contiguous tube voltages and thus similar noise levels. Additionally, lower kV settings are desirable in thin or adolescent patients.

Gold is currently used to treat rheumatoid arthritis either orally or by intramuscular injection [15]. Gold nanoparticles were introduced as a potential X-ray contrast agent in 2006 [16]. The K-edge of gold (81 keV) might theoretically allow material differentiation using 80 and 100 kV spectra. The attenuation of iodine and gold at different photon energy levels is visualized in **Figure 1**. The aim of this *in vitro* study was to compare the differentiation of iodine and gold from body tissues in DECT using different kV spectra. To our best knowledge, this is the first study evaluating gold as a potential DECT contrast agent.

2. Materials and Methods

2.1. Phantom Setup

A 3 ml syringe filled with sodium aurothiomalate with a concentration of 50 mg/ml (Tauderon 50, Altana Pharma, Germany), corresponding to a concentration of 22.65 mg gold per ml, was used as gold specimen. Another 3 ml syringe filled with saline diluted iopamidol (Iomeron 300, Bracco Imaging S.p.A., Italy) with an iodine concentra-

tion of 50 mg/ml was used as iodine specimen. The concentration of gold was given by the highest available therapeutic concentration of sodium aurothiomalate. The 50 mg/ml concentration of iodine was chosen in a preceding test series with different iodine concentrations to achieve attenuation similar to the gold compound at middle tube voltage settings (100 kV and 120 kV). Porcine thigh bone was used as bone specimen. Lean pork loin muscle was used as muscle specimen. The specimens were positioned in a water filled tank with a size of $19 \times 14 \times 23$ cm³.

2.2. Scanning Protocols

All scans were performed using a dual source CT (Somatom Definition, Siemens Healthcare, Forchheim, Germany). To ensure the direct comparability between all four datasets, we decided to acquire four consecutive datasets with the same tube/detector combination (single-source mode) instead of acquiring two datasets simultaneously (e.g. 80 kV on tube A and 140 kV on tube B), which would also be possible. No changes were expected within the short time intervals between the consecutive scans of a static phantom. Consecutive scans with 80 kV, 100 kV, 120 kV and 140 kV tube voltage settings were performed. All

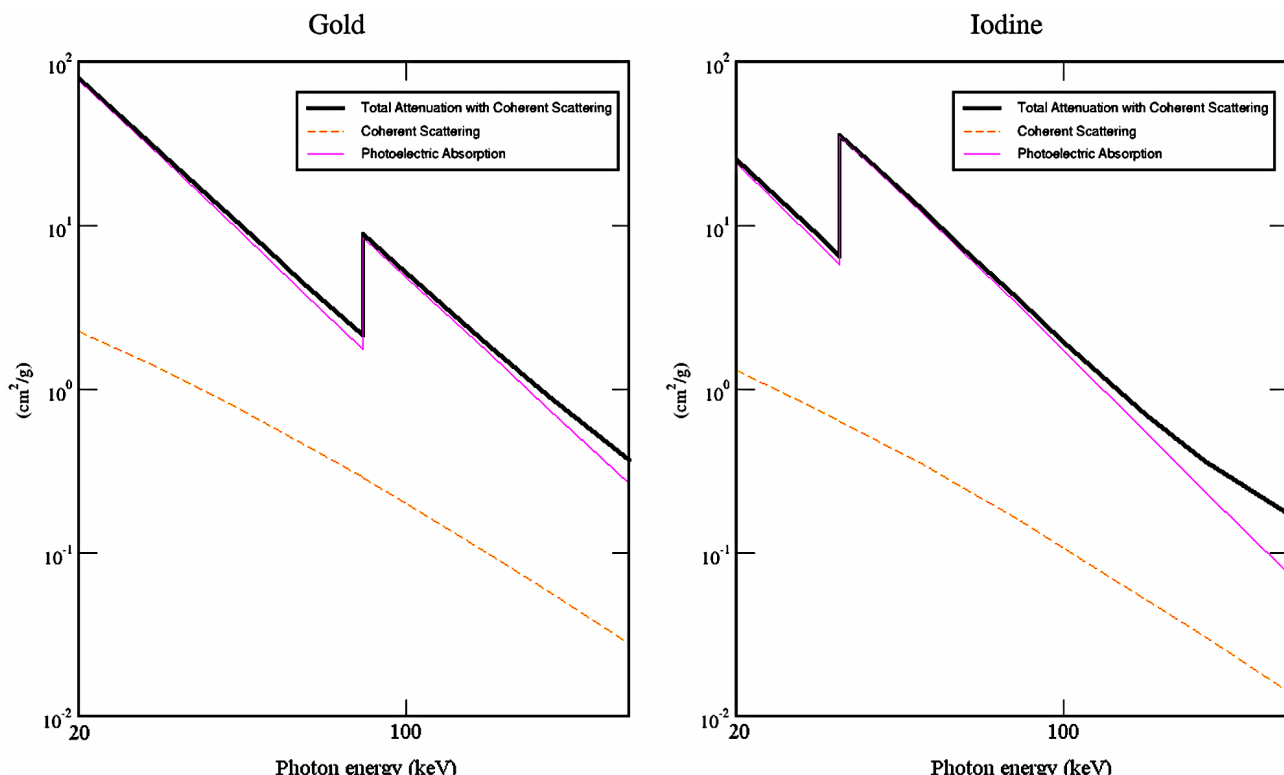


Figure 1. Attenuation of gold and iodine at different photon energies with the components photoelectric absorption and coherent scattering. Note the abrupt increase in total attenuation at the K edge. The K edge of iodine at 33.2 keV is below the presently used energy spectrum of diagnostic CT. The K edge of gold at 80.7 keV is localized within the energy spectrum of diagnostic CT. Data courtesy of XCOM Photon Cross Sections Database [28].

other scan parameters were constant for all four tube voltage settings: 210 mA reference tube current time product with automatic tube current modulation (CARE Dose 4D), 0.5 s gantry rotation time, and $32 \times 0.6\text{-mm}$ collimation with z-flying focal spot. The images were reconstructed with a non edge enhancing B30 kernel. Slice thickness and increment were 5 mm and 4 mm respectively, and the reconstructed field of view was 205 mm with a 512×512 pixel matrix. The volume CT dose index (CTDI_{vol}) and dose length product (DLP) were recorded.

2.3. Density Measurements and DE Ratio

All measurements were performed on a PACS workstation (OsiriX Pro, Aycan, Rochester, NY). The software allows to copy a region of interest (ROI) between different series windows. As all other settings and reconstruction parameters except the kV-settings remained unchanged between the datasets, it was possible to copy a manually drawn ROI from the 80 kV data set to the exact same position in the three higher kV datasets. Thus, the mean density (HU) measurements were directly comparable. The iodine and gold ROIs were circular and had a size of 170 pixels. The muscle ROI was elliptical and had a size of 800 pixels. The compact bone ROI was of polyangular shape and had a size of 750 pixels.

DE_{ratio} of the different materials were computed by dividing the mean HU value of the low-energy data set by the mean high energy HU value [17]:

$$\text{DE}_{\text{ratio}} = \text{HU}_{\text{low kV}} / \text{HU}_{\text{high kV}},$$

where low is 80 kV and high is 100, 120 or 140 kV

Since the ability to discriminate between different materials in DECT depends primarily on the difference in DE_{ratio} , any increase is expected to improve the performance of any material-specific DECT imaging task. Therefore, analogous to a phantom study performed by Primak *et al.* [13], we calculated the difference between material specific DE_{ratio} to compare the ability of discrimination between materials.

3. Results

The mean attenuation values of iodine, gold, compact bone, and muscle at different X-ray tube kVp spectra are summarized in **Table 1** together with the corresponding calculated DE_{ratio} . The attenuation of gold increased compared to 80 kVp at higher kVp-settings, while the attenuation of all other specimens decreased. This results in $\text{DE}_{\text{ratio}} < 1$ for gold. The mean attenuation values of iodine and gold were almost identical at 100 kVp. The attenuation of iodine was 47% higher at 80 kV, and 29% lower at 140 kVp in comparison to gold. The attenuation of gold and iodine at different energy spectra is shown in

Figure 2. There was only a mild decrease of the mean attenuation values of muscle with increasing kVp-settings, resulting in $\text{DE}_{\text{ratio}} \sim 1$.

The differences between the DE_{ratio} of the specimens at different kVp combinations are summarized in **Table 2**. The differences between DE_{ratio} of gold and bone were higher than those of iodine and bone for all tube voltage combinations. The highest difference in DE_{ratio} between bone and gold of 0.53 was found at a tube voltage combination of 80/140 kVp (bone and iodine 0.46). A relatively high difference in DE_{ratio} between bone and gold was already seen at low tube voltage combination of 80/100 kVp. The differences between DE_{ratio} of gold and muscle were conversely lower than those of iodine and muscle (0.83 for iodine and muscle and 0.16 for gold and muscle at 80/140 kVp).

The volume CT dose index (CTDI_{vol}) and dose length product (DLP) of the four scans with a constant scan length are summarized in **Table 3**.

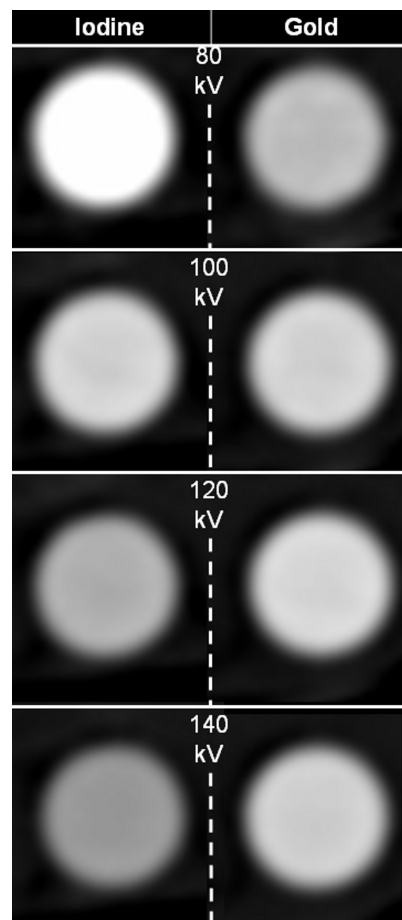


Figure 2. Attenuation of iodine and gold at different x-ray tube kVp spectra (window width 1700 HU, window level 700 HU). The attenuation of iodine decreases continuously with increasing kVp. The attenuation of gold increases visibly from 80 kVp to 100 kVp and remains quite stable from 100 kVp to 140 kVp.

Table 1. Mean attenuation values and standard deviations of iodine, gold, compact bone, and muscle at different X-ray tube kVp spectra. DE_{ratios} with 95% confidence intervals calculated from the mean attenuation values for different X-ray tube kVp spectra combinations.

| | 80 kVp (HU) | 100 kVp (HU) | 120 kVp (HU) | 140 kVp (HU) | DE ratio 80/100 kVp | DE ratio 80/120 kVp | DE ratio 80/140 kVp |
|-------------------------------|-------------|--------------|--------------|--------------|------------------------------|------------------------------|------------------------------|
| Iodine (50 mg/ml) | 1651 ± 27 | 1261 ± 23 | 1017 ± 21 | 864 ± 16 | 1.31 (1.30 - 1.31) | 1.62 (1.62 - 1.63) | 1.91 (1.90 - 1.92) |
| Gold (22.65 mg/ml) | 1120 ± 18 | 1251 ± 14 | 1275 ± 17 | 1218 ± 16 | 0.89 (0.89 - 0.90) | 0.88 (0.88 - 0.88) | 0.92 (0.92 - 0.92) |
| Compact bone | 1732 ± 299 | 1441 ± 263 | 1245 ± 239 | 1195 ± 198 | 1.20 (1.18 - 1.22) | 1.39 (1.37 - 1.42) | 1.45 (1.42 - 1.47) |
| Muscle | 69 ± 5 | 68 ± 5 | 67 ± 3 | 64 ± 3 | 1.01 (1.01 - 1.02) | 1.03 (1.02 - 1.04) | 1.08 (1.07 - 1.08) |

Table 2. Absolute differences between DE_{ratios} of iodine or gold and compact bone or muscle for different X-ray tube kVp spectra combinations.

| | 80/100 kVp | 80/120 kVp | 80/140 kVp |
|--------------------------------|------------|------------|------------|
| Iodine and compact bone | 0.11 | 0.23 | 0.46 |
| Gold and compact bone | 0.31 | 0.51 | 0.53 |
| Iodine and muscle | 0.29 | 0.59 | 0.83 |
| Gold and muscle | 0.12 | 0.15 | 0.16 |

Table 3. Volume CT dose index (CTDI_{vol}) and dose length product (DLP) of the consecutive CT scans of the phantom with increasing X-ray tube kVp spectra.

| kVp | CTDI vol (mGy) | DLP (mGy·cm) |
|------------|----------------|--------------|
| 80 | 1.01 | 9 |
| 100 | 2.34 | 22 |
| 120 | 4.31 | 40 |
| 140 | 6.68 | 62 |

4. Discussion

In this *in vitro* study, we could demonstrate that the 81 keV K-edge of gold impacts the attenuation of a low concentrated gold compound solution scanned by energy spectra of diagnostic CT. The attenuation of gold increased slightly compared to 80 kVp at higher kVp-settings, while the attenuation of all other specimens decreased.

Relevant differences in DE_{ratios} between bone and gold were seen at all tube voltage combinations, mentionable with a contiguous low tube voltage combination of 80 kV and 100 kV. This would be advantageous in DECT applications where differentiation between contrast agent and bone is the major goal, e.g., bone removal in post-processing at head and neck CTA [18,19] or CTA runoff [20,21]. These exams could be performed with contiguous low tube voltages, resulting in lower radiation dose. Alternatively, the differentiation between bone and contrast agent might be more precise with a 80/140 kV combination.

As already shown in numerous previous studies, the attenuation of muscle decreases only slightly with increasing tube voltage settings [2,4,10]. This resulted in

small differences between the DE_{ratios} of gold and muscle in our study. Thus, in DECT applications where differentiation between contrast agent and soft tissue is the major goal, e.g. virtual non-contrast image calculation [22,23], iodine should be more advantageous for all tube voltage combinations.

The concentration of iodine was more than twice the concentration of gold in our study (50 mg/ml versus 22.65 mg/ml). As mentioned in the methods part, the concentration of iodine was adapted to achieve attenuation similar to the gold compound at middle tube voltage settings (100 kV and 120 kV). With a higher atomic number (Gold = 79 vs Iodine = 53), and a higher absorption coefficient, gold should theoretically provide about 2.7 times greater contrast per unit weight than iodine [16]. Extrapolating the concentrations in our study, a contrast agent with a gold concentration of about 136 mg/ml might be equivalent to a 300 mg/ml iodine contrast agent at 100 kV.

Tin filtration of the high energy (140 kVp) tube was introduced with the second generation of dual-source CT. This can further improve DE material discrimination [13, 24]. Our first generation dual source CT does not provide any additional filtration options. Therefore, filtration effects could not be investigated in our study. Our hypothesis is that filtration of the low energy tube (80 kVp) might enhance the K-edge effect of gold scanned by energy spectra of diagnostic CT.

In DECT imaging, mAs-settings are routinely decreased with higher kVp-settings to obtain similar noise levels in both datasets. All scans were performed with the same mAs in our study. However, the mAs was selected high enough to perform reliable attenuation measurements in all datasets. Our intention was to keep all other parameters except kVp constant.

The major limitation of gold as a potential DECT contrast agent might be its well known side effects. Sodium aurothiomalate is a gold compound that is used for its antirheumatic effects to treat rheumatoid arthritis and for some experimental indications (e.g. of prostate cancer) [15,25]. This compound causes allergic reaction frequently, and can impair nephrogenic or hematopoietic function with higher dose [15]. Thus, it is not eligible as a contrast

agent. Gold nanoparticles were developed and introduced in 2006 as a potential X-ray contrast agent in a small animal study [16]. A negligible osmolarity, a low viscosity, no evidence of toxicity, and extended imaging time were highlighted as the advantages of this novel contrast agent [16]. Initial *in vitro* CT studies could demonstrate a good performance of gold nanoparticles with high tube voltage, large objects (patients) or strong added filtration [26,27]. In our feasibility study, we wanted to investigate the potential of gold in DECT. For proof of principle of our *in vitro* experiment, we considered sodium aurothiomalate advantageous for its availability and its lower costs.

Especially the high costs could limit the wider spread of gold as a contrast agent. The gold price was rising within the past years and was about 54\$/g in 2012. Assuming a standard injection of 100 ml of a contrast agent with a 136 mg/ml gold concentration, the raw material cost would be about 735\$ per patient. Such high cost would only be legitimate in certain patient groups. A potential group might be patients with known allergy versus iodine contrast agents. Another potential group might be children or thin patients, where low kilovoltage DECT scans are desirable to reduce the radiation dose.

In conclusion, DE_{ratio} of gold remains relatively stable along the energy spectrum of diagnostic CT and allows a reliable material differentiation between gold and bone already at contiguous low tube voltage settings (80 kV and 100 kV). Thus, gold might have a potential as a contrast agent for certain DECT applications.

REFERENCES

- [1] D. E. Avrin, A. Macovski and L. E. Zatz, "Clinical Application of Compton and Photo-Electric Reconstruction in Computed Tomography: Preliminary Results," *Investigative Radiology*, Vol. 13, No. 3, 1978, pp. 217-222. <http://dx.doi.org/10.1097/00004424-197805000-00007>
- [2] T. R. Johnson, B. Krauss, M. Sedlmair, M. Grasruck, H. Bruder, D. Morhard, C. Fink, S. Weckbach, M. Lenhard, B. Schmidt, T. Flohr, M. F. Reiser and C. R. Becker, "Material Differentiation by Dual Energy CT: Initial Experience," *European Radiology*, Vol. 17, No. 6, 2007, pp. 1510-1517. <http://dx.doi.org/10.1007/s00330-006-0517-6>
- [3] R. A. Kruger, S. J. Riederer and C. A. Mistretta, "Relative Properties of Tomography, K-Edge Imaging, and K-Edge Tomography," *Medical Physics*, Vol. 4, No. 3, 1977, pp. 244-249. <http://dx.doi.org/10.1118/1.594374>
- [4] W. Huda, E. M. Scalzetti and G. Levin, "Technique Factors and Image Quality as Functions of Patient Weight at Abdominal CT," *Radiology*, Vol. 217, No. 2, 2000, pp. 430-435.
- [5] Y. Nakayama, K. Awai, Y. Funama, M. Hatemura, M. Imuta, T. Nakaura, D. Ryu, S. Morishita, S. Sultana, N. Sato and Y. Yamashita, "Abdominal CT with Low Tube Voltage: Preliminary Observations about Radiation Dose, Contrast Enhancement, Image Quality, and Noise," *Radiology*, Vol. 237, No. 3, 2005, pp. 945-951. <http://dx.doi.org/10.1148/radiol.2373041655>
- [6] G. N. Hounsfield, "Computerized Transverse Axial Scanning (Tomography). 1. Description of System," *British Journal of Radiology*, Vol. 46, No. 552, 1973, pp. 1016-1022. <http://dx.doi.org/10.1259/0007-1285-46-552-1016>
- [7] S. J. Riederer and C. A. Mistretta, "Selective Iodine Imaging Using K-Edge Energies in Computerized X-Ray Tomography," *Medical Physics*, Vol. 4, No. 6, 1977, pp. 474-481. <http://dx.doi.org/10.1118/1.594357>
- [8] L. M. Zatz, "The Effect of the kVp Level on EMI Values. Selective Imaging of Various Materials with Different kVp Settings," *Radiology*, Vol. 119, No. 3, 1976, pp. 683-688.
- [9] P. R. Seidensticker and L. K. Hofmann, "Dual Source CT Imaging," Springer Medizin Verlag, Heidelberg, 2008. <http://dx.doi.org/10.1007/978-3-540-77602-4>
- [10] T. G. Flohr, C. H. McCollough, H. Bruder, M. Petersilka, K. Gruber, C. Suss, M. Grasruck, K. Stierstorfer, B. Krauss, R. Raupach, A. N. Primak, A. Kuttner, S. Achenbach, C. Becker, A. Kopp and B. M. Ohnesorge, "First Performance Evaluation of a Dual-Source CT (DSCT) System," *European Radiology*, Vol. 16, No. 2, 2006, pp. 256-268. <http://dx.doi.org/10.1007/s00330-005-2919-2>
- [11] Y. H. Lee, K. K. Park, H. T. Song, S. Kim and J. S. Suh, "Metal Artefact Reduction in Gemstone Spectral Imaging Dual-Energy CT with and without Metal Artefact Reduction Software," *European Radiology*, Vol. 22, No. 6, 2012, pp. 1331-1340. <http://dx.doi.org/10.1007/s00330-011-2370-5>
- [12] J. P. Schломka, E. Roessl, R. Dorschied, S. Dill, G. Martens, T. Istel, C. Baumer, C. Herrmann, R. Steadman, G. Zeitler, A. Livne and R. Proksa, "Experimental Feasibility of Multi-Energy Photon-Counting K-Edge Imaging in Pre-Clinical Computed Tomography," *Physics in Medicine & Biology*, Vol. 53, No. 15, 2008, pp. 4031-4047. <http://dx.doi.org/10.1088/0031-9155/53/15/002>
- [13] A. N. Primak, J. C. Ramirez Giraldo, X. Liu, L. Yu and C. H. McCollough, "Improved Dual-Energy Material Discrimination for Dual-Source CT by Means of Additional Spectral Filtration," *Medical Physics*, Vol. 36, No. 4, 2009, pp. 1359-1369. <http://dx.doi.org/10.1118/1.3083567>
- [14] M. Karcaaltincaba and A. Aktas, "Dual-Energy CT Revisited with Multidetector CT: Review of Principles and Clinical Applications," *Diagnostic and Interventional Radiology*, Vol. 17, No. 3, 2011, pp. 181-194.
- [15] J. D. Jessop, M. M. O'Sullivan, P. A. Lewis, L. A. Williams, J. P. Camilleri, M. J. Plant and E. C. Coles, "A Long-Term Five-Year Randomized Controlled Trial of Hydroxychloroquine, Sodium Aurothiomalate, Auranofin and Penicillamine in the Treatment of Patients with Rheumatoid Arthritis," *British Journal of Rheumatology*, Vol. 37, No. 9, 1998, pp. 992-1002. <http://dx.doi.org/10.1093/rheumatology/37.9.992>
- [16] J. F. Hainfeld, D. N. Slatkin, T. M. Focella and H. M. Smilowitz, "Gold Nanoparticles: A New X-Ray Contrast Agent," *British Journal of Radiology*, Vol. 79, No. 939, 2006, pp. 248-253. <http://dx.doi.org/10.1259/bjr/13169882>

- [17] D. T. Boll, N. A. Patil, E. K. Paulson, E. M. Merkle, W. N. Simmons, S. A. Pierre and G. M. Preminger, "Renal Stone Assessment with Dual-Energy Multidetector CT and Advanced Postprocessing Techniques: Improved Characterization of Renal Stone Composition—Pilot Study," *Radiology*, Vol. 250, No. 3, 2009, pp. 813-820. <http://dx.doi.org/10.1148/radiol.2503080545>
- [18] D. Morhard, C. Fink, A. Graser, M. F. Reiser, C. Becker and T. R. Johnson, "Cervical and Cranial Computed Tomographic Angiography with Automated Bone Removal: Dual Energy Computed Tomography versus Standard Computed Tomography," *Investigative Radiology*, Vol. 44, No. 5, 2009, pp. 293-297. <http://dx.doi.org/10.1097/RLI.0b013e31819b6fba>
- [19] L. J. Zhang, S. Y. Wu, C. S. Poon, Y. E. Zhao, X. Chai, C. S. Zhou and G. M. Lu, "Automatic Bone Removal Dual-Energy CT Angiography for the Evaluation of Intracranial Aneurysms," *Journal of Computer Assisted Tomography*, Vol. 34, No. 6, 2010, pp. 816-824. <http://dx.doi.org/10.1097/RCT.0b013e3181eff93c>
- [20] C. Brockmann, S. Jochum, M. Sadick, K. Huck, P. Ziegler, C. Fink, S. O. Schoenberg and S. J. Diehl, "Dual-Energy CT Angiography in Peripheral Arterial Occlusive Disease," *CardioVascular and Interventional Radiology*, Vol. 32, No. 4, 2009, pp. 630-637. <http://dx.doi.org/10.1007/s00270-008-9491-5>
- [21] B. C. Meyer, T. Werncke, W. Hopfenmuller, H. J. Raatschen, K. J. Wolf and T. Albrecht, "Dual Energy CT of Peripheral Arteries: Effect of Automatic Bone and Plaque Removal on Image Quality and Grading of Stenoses," *European Journal of Radiology*, Vol. 68, No. 3, 2008, pp. 414-422. <http://dx.doi.org/10.1016/j.ejrad.2008.09.016>
- [22] A. Graser, T. R. Johnson, H. Chandarana and M. Macari, "Dual Energy CT: Preliminary Observations and Potential Clinical Applications in the Abdomen," *European Journal of Radiology*, Vol. 19, No. 1, 2008, pp. 13-23.
- [23] M. Toepker, T. Moritz, B. Krauss, M. Weber, G. Euller, T. Mang, F. Wolf, C. J. Herold and H. Ringl, "Virtual Non-Contrast in Second-Generation, Dual-Energy Computed Tomography: Reliability of Attenuation Values," *European Journal of Radiology*, Vol. 81, No. 3, 2012, pp. e398-e405. <http://dx.doi.org/10.1016/j.ejrad.2011.12.011>
- [24] C. Thomas, B. Krauss, D. Ketelsen, I. Tsiflikas, A. Reimann, M. Werner, D. Schilling, J. Hennenlotter, C. D. Claussen, H. P. Schlemmer and M. Heuschmid, "Differentiation of Urinary Calculi with Dual Energy CT: Effect of Spectral Shaping by High Energy Tin Filtration," *Investigative Radiology*, Vol. 45, No. 7, 2010, pp. 393-398.
- [25] M. Trani, A. Sorrentino, C. Busch and M. Landstrom, "Pro-Apoptotic Effect of Aurothiomalate in Prostate Cancer Cells," *Cell Cycle*, Vol. 8, No. 2, 2009, pp. 306-313. <http://dx.doi.org/10.4161/cc.8.2.7596>
- [26] M. W. Galper, M. T. Saung, V. Fuster, E. Roessl, A. Thran, R. Proksa, Z. A. Fayad and D. P. Cormode, "Effect of Computed Tomography Scanning Parameters on Gold Nanoparticle and Iodine Contrast," *Investigative Radiology*, Vol. 47, No. 8, 2012, pp. 475-481. <http://dx.doi.org/10.1097/RLI.0b013e3182562ab9>
- [27] T. Nowak, M. Hupfer, R. Brauweiler, F. Eisa and W. A. Kalender, "Potential of High-Z Contrast Agents in Clinical Contrast-Enhanced Computed Tomography," *Medical Physics*, Vol. 38, No. 12, 2011, pp. 6469-6482. <http://dx.doi.org/10.1118/1.3658738>
- [28] M. J. Berger, J. H. Hubbell, S. M. Seltzer, J. Chang, J. S. Coursey, R. Sukumar, D. S. Zucker and K. Olsen, "XCOM: Photon Cross Sections Database," 1998. <http://www.nist.gov/pml/data/xcom/index.cfm>